AIMS Biophysics, 4(1): 43-62.
DOI: 10.3934/biophy.2017.1.43
Received: 28 August 2016
Accepted: 13 December 2016
Published: 27 December 2016

http://www.aimspress.com/journal/biophysics

Review

Towards understanding of plant mitochondrial VDAC proteins: an overview of bean (*Phaseolus*) VDAC proteins

Hayet Saidani [1], Daria Grobys [2], Marc Léonetti [3], Hanna Kmita [2] and Fabrice Homblé [1,*]

[1] Structure et Fonction des Membranes Biologiques, Université Libre de Bruxelles (ULB), Boulevard du Triomphe CP 206/2, B-1050 Brussels, Belgium
[2] Laboratory of Bioenergetics, Institute of Molecular Biology and Biotechnology, Faculty of Biology, Adam Mickiewicz University, Umultowska 89, 61-614 Poznan, Poland
[3] I.R.P.H.E., Aix-Marseille Université, CNRS, Technopôle de Château-Gombert, F-13384, Marseille Cedex 13, France

* **Correspondence:** Email: fhomble@ulb.ac.be.

Abstract: As the main grain legume consumed worldwide, the common bean (*Phaseolus vulgaris*) is generally considered as a model for food legumes. The mitochondrial voltage-dependent anion-selective channel (VDAC) is the major transport pathway for inorganic ions, metabolites, and tRNA, and consequently it controls the exchange of these compounds between the cytoplasm and the mitochondrion. Two VDAC isoforms of *Phaseolus coccineus* have been investigated experimentally. However, plant VDACs are known to belong to a small multigenic family of variable size. Here, we combine available experimental as well as genomic and transcriptomic data to identify and characterize the VDAC family of *Phaseolus vulgaris*. To this aim, we review the current state of our knowledge of Phaseolus VDAC functional and structural properties. The genomic and transcriptomic data available for the putative VDACs of *Phaseolus vulgaris* are studied using bioinformatics approach including homology modelling. The obtained results indicate that five out of the seven putative VDAC encoding sequences (named PvVDAC1–5) share strongly conserved motifs and structural homology with known VDACs. Notably, PvVDAC4 and PvVDAC5 are very close to the two abundant and characterized experimentally VDAC isoforms purified from *Phaseolus coccineus* mitochondria.

Keywords: Phaseolus; mitochondria; VDAC; functional and structural properties

1. Introduction

A big societal challenge is to increase the yields of crop plants without detrimental impact on the environment. Among the major crops, seed crops are one of the main sources for human sustenance (http://www.fao.org/docrep/007/y5609e/y5609e02.htm). In this respect, plants like the common bean representing the genus Phaseolus are very attractive as they are able to fix atmospheric nitrogen. The genus Phaseolus contains five domesticated species with distinct traits: common bean (*Phaseolus vulgaris L.*), runner bean (*Phaseolus coccineus L.*), lima bean (*Phaseolus. lunatus L.*), tepary bean (*Phaseolus. acutifolius A*. Gray), and year bean (*Phaseolus. polyanthus* Greenman). *P. coccineus* is closely related to *P. vulgaris* and it is the most important grain legume consumed worldwide for its edible seeds and pods [1,2].

The seed development can be divided into three phases: (1) the embryo biogenesis, differentiation and histodifferentiation stage, which occurs with a slow increase in biomass rate, (2) the maturation and filling stage featuring an intense metabolism and a huge biomass increase and (3) the desiccation stage. Recently, a proteomic study performed for the stages, from late embryogenesis to seed desiccation, has highlighted the dynamics of the protein profile during the development of *P. vulgaris* seeds [3]. An increased proportion of proteins involved in the general metabolism including the tricarboxylic acid cycle and glycolysis as well as DNA and RNA metabolisms characterizes the first stage. The active synthesis of storage macromolecules occurs during the second stage while in the last one, the energy transformation is slow down and the synthesis of proteins related to the oxidation/reduction processes increases. Early physiological studies on *P. lunatus* seeds show the correlation between the initial rate of respiration and seed germination [4]. The seed germination starts with a relatively fast growth, which implies a high requirement of catabolism based on large storage macromolecules, mainly proteins and starch, as well as anabolism, i.e. de novo synthesis of proteins, lipids and sugar polymers as well as other metabolites required for the growth and development of the plant.

The intensive respiratory and metabolic activity observed during both seed development and germination requires an efficient exchange of metabolites between the mitochondrial matrix and the cytoplasm. This exchange involves transport of solutes through the mitochondrial outer and inner membranes (MOM and MIM, respectively), Several specific transporters that belong to the mitochondrial carrier family (MCF) [5], potassium channels [6,7,8] and ABC transporters [9,10] enable to transport solutes through MIM. The voltage-dependent anion-selective channel (VDAC) is the major pathway for metabolite (e.g., ATP) and ion transport through MOM. As such, it may have central role in the regulation of mitochondrial and cell metabolism and thereby in the seed development and germination. Despite the fact that VDAC is a predominant proteins of MOM, there is growing evidence indicating its extra-mitochondrial localization [11]. For instance, three out of the four VDAC isoforms of *Arabidopsis thaliana*, i.e. AtVDAC1, AtVDAC2 and AtVDAC3, may be targeted to both mitochondria and the plasma membrane (PM), and the latter one is the most abundant in PM [12,13]. The PM localization was also shown for VDAC1 in mammalian cells [14,15]. The function of plant VDAC in PM is so far unknown. For mouse cells, it has been suggested that VDAC1 could function as a redox enzyme [16] although, the mechanism underpinning this function remains to be elucidated.

The first evidence of plant VDAC dates back from the sixties of the 20th century when electron microscopy studies on *P. aureus* mitochondria showed the presence in MOM of large (2.5–3.0 nm in

diameter) "pits" [17]. Then, it has been shown that the "pits" co-occur at a high surface density (2×10^4 protein/μm^2) with a 30 kDa protein [18] that is permeable to a polymer of about 5 kDa [19]. The protein was then purified from mitochondria of various plants and its typical VDAC features were detected by electrophysiology [11]. Moreover, a protein, named PcVDAC32, in reference to its apparent molecular mass, was purified from *P. coccineus* seeds and was used for both structural and functional studies [11]. Importantly, *P. vulgaris* genome and transcriptome sequence availability [20] enables to get insight into specific features of the different VDAC isoforms in this genus. As the main grain legume consumed worldwide, the common bean (*P. vulgaris*) is generally considered as a model for food legumes. In parallel to the genetic improvement made to increase their agricultural and food quality, efforts should be undertaken to understand their physiology at a molecular level.

Mitochondria are the place of ATP required for cell metabolism and contribute to plant response to biotic and abiotic stresses. Genetic modifications that improve some plant trait should also preserved or enhanced the mitochondrial function notably to avoid adverse consequence in cell bioenergetics and in plant resistance to environmental clues. VDAC plays a key role in the exchange of ions and metabolites (e.g., ATP, ADP, NADH, succinate, malate, tRNA) between the cytosol and mitochondria [11]. Importantly, there is a growing number of data indicating a role of VDAC in stress-induced regulated cell death in plant cells. The molecular mechanisms underpinning the phenomenon are still elusive. As VDAC plays a central role at the cytoplasm-mitochondrial interface, it is of prime importance to identify its various isoforms that are expressed in different plants, to study their expression, to decipher their structure-function relationship and to understand regulating mechanisms. In this framework, we provide here the current state of our knowledge of *Phaseolus* VDAC functional and structural properties hoping that it will pave the way for future research.

2. Functional Features

Two VDAC isoforms were purified from seeds of *Phaseolus coccineus* var. streamlined and named PcVDAC32 and PcVDAC31 at the basis of their apparent molecular mass estimated by SDS-PAGE [21]. It has been shown that PcVDAC32 is three times more abundant than PcVDAC31 but they have the same channel activity [21] and overall secondary structure [22]. Moreover, in two-dimensional gels PcVDAC32 and PcVDAC31 isoforms migrate as two polypeptides with pI of 7.6 and 8.8, respectively that permits their separation by chromatofocusing. In addition, the two isoforms display a different proteolytic pattern upon limited digestion with the protease V8 from *Staphylococcus aureus* that suggests a significant difference in their amino acid sequence [21]. Because of its greater abundance and because of the possibility to purify PcVDAC32, this isoform was chosen for functional studies.

The functional properties of VDAC are usually studied by electrophysiology after reconstitution of one or several proteins in a planar lipid bilayer for single channel or multichannel analysis, respectively [23]. Channels are usually characterized by their conductance, selectivity and gating. The conductance reflects the rate of ion flow through a channel. In a salt concentration close to that found in vivo (0.1 M) PcVDAC32 open state has a conductance of ~0.4 nS (Figure 1). The conductance increases linearly with KCl concentration (Figure 2), suggesting the absence of binding site for K^+ and Cl^- ions.

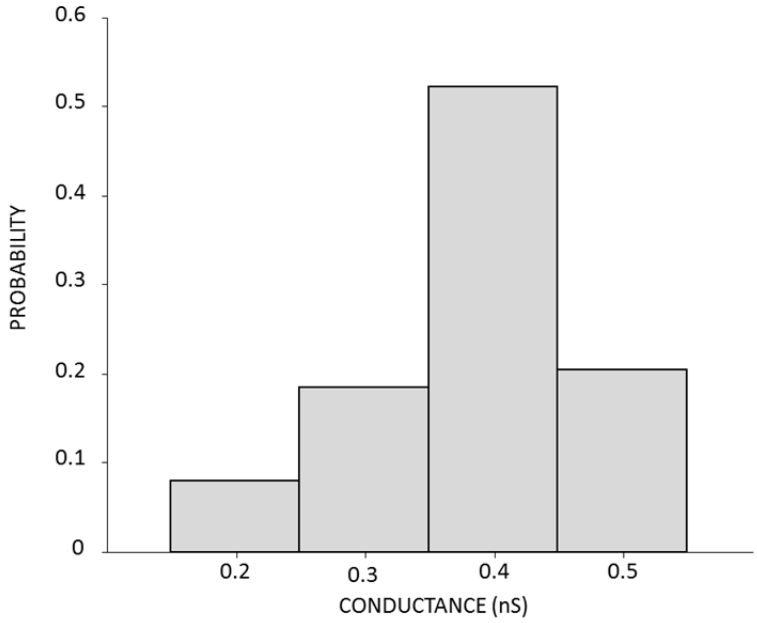

Figure 1. PcVDAC32 single channel conductance at the open state (n = 259) recorded in 0.1M KCl buffered with 10 mM HEPES (pH = 7.5). See [23,24] for methodological details.

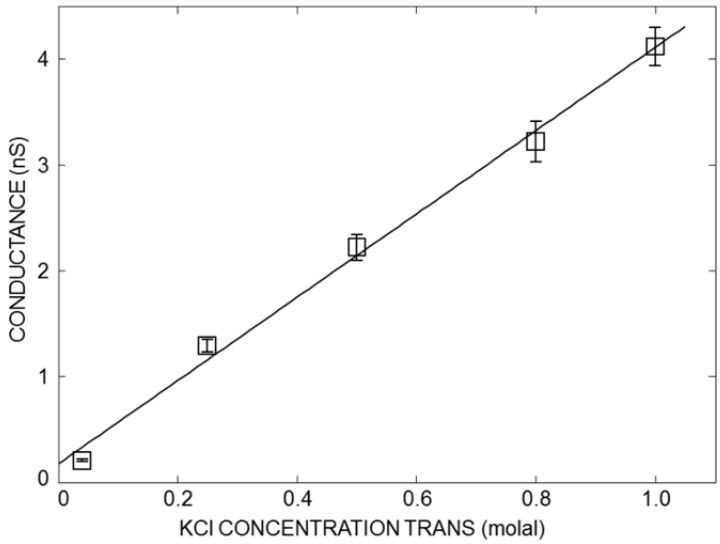

Figure 2. Effect of KCl concentration on PcVDAC32 single channel conductance at the open state. KCl solutions were buffered with 10 mM HEPES (pH = 7.5). A linear least square regression was used to fit the data (R^2 = 0.995). See [23,24] for methodological details.

For historical reason the conductance of VDAC channels is usually recorded in 1 M KCl. At this concentration, the open state conductance is nearly equal for various studied plant VDACs (Table 1). The open state selectivity of VDAC is weak. Nonetheless, its permeability towards

inorganic anions is higher than that of inorganic cations (Table 1). This is consistent with its transport function since most metabolites flowing through VDAC are negatively charged (e.g., ATP^4, ADP^{3-}, $succinate^{2-}$). VDAC is referred to as voltage-dependent because it usually switches from the fully open state to subconductance states in the presence of a difference in membrane electric potential (membrane potential $|V| \geq 20$ mV, where $|V|$ denotes the absolute value). A typical transition of a single channel from the open state to subconductance states is shown in (Figure 3A). It occurs at both positive and negative membrane potentials. In multichannel experiments the voltage-dependence features a symmetrical bell shape (Figure 3B). It can be quantified by plotting the change in the relative conductance of the membrane as a function of the applied voltage [24,25] and using the Boltzmann distribution: $\ln (P_o(V)/(1 - P_o(V)) = \pm ne(V - V_h)/kT$ where $P_o(V)$ is the probability of occurrence of the open state, V_h is the voltage at which half of the channels are in their open state, n is a measure of the steepness of the voltage dependence, V is the voltage applied across the membrane, *e* is the elementary charge, k is the Boltzmann constant and T is the absolute temperature. $P_o(V)$ is calculated from the relative change in membrane conductance: $P_o(V) = (G(V) - G_{min})/(G_{max} - G_{min})$, where G_{max} and G_{min} are the maximal and the minimal conductance, respectively. G_{max} is obtained at low applied voltages ($|V| < 20$ mV) when the channels are predominately in the fully open state and G_{min} is calculated at high applied voltages ($|V| > 50$mV) when the channels switch to subconductance states. The values of n and V_h calculated for PcVDAC32 are 2.5 and 27 mV, respectively [24]. When the reconstituted VDAC undergo transition from the open state to subconductance states, the change in the membrane conductance is about 30% (Figure 3B). The magnitude of the conductance change depends on the membrane lipid composition and salt concentration [24].

Table 1. The open state conductance and selectivity of VDAC purified from mitochondria of various plant species.

Plant	Conductance (nS)	Selectivity: P_{Cl}/P_K	References
Phaseolus coccineus	3.7–4	2	[21]
Pisum sativum	3.7	1.4	[27]
Solanum tuberosum	3.5	1.7	[28]
Triticum aestivum	4.1	2	[29]
Zea mais	3.6–3.9	1.2–1.7	[30,31]

The voltage-mediated change in PcVDAC32 conductance is usually correlated to a reverse selectivity, i.e. the channel becomes cation selective in the subconductance states (up to $P_K/P_{Cl} \sim 40$ in the presence of a fivefold KCl gradient) [21]. The fact that PcVDAC32 adopts switchable states with opposite selectivity suggests that, as VDAC of other organisms, it might control the metabolite exchanges through MOM. In support of this assumption, it is worth noting that *Neurospora crassa* VDAC is permeable to ATP in the open state but not after switching to a subconductance state [26].

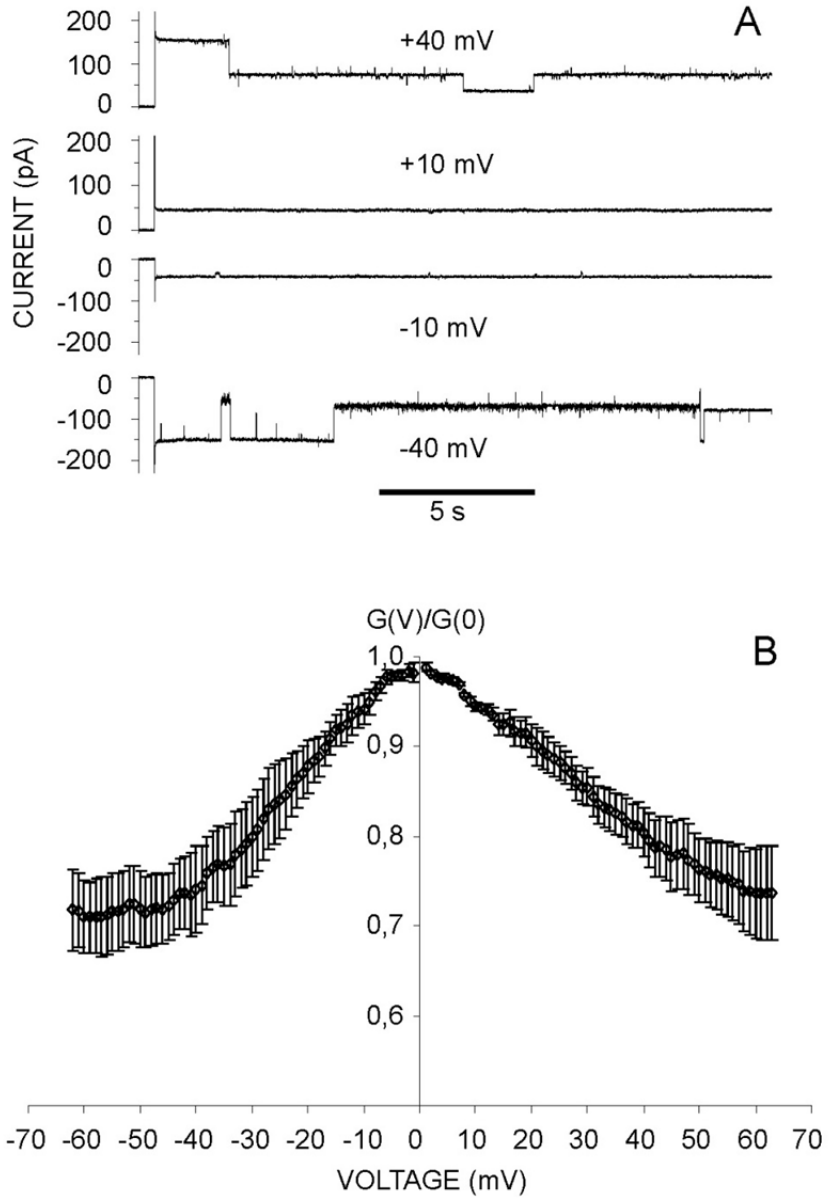

Figure 3. The voltage dependence of PcVDAC32. (A) Single channel recordings showing transition to subconductance states at $|V| \geqslant 10$ mV. (B) Changes in the relative conductance due to the applied voltage in a multichannel experiment. Data were recorded in the presence of 1M KCl buffered with 10 mM HEPES (pH = 7.5). See [23,24] for methodological details.

A large number of VDAC proteins purified from mitochondria of organisms representing different phylogenetic groups share the same fundamental properties in respect to the conductance, selectivity and voltage dependence. Thus, despite the low similarity of their amino acid sequence [11], their basic functional properties are conserved in the course of evolution although this does not exclude the existence of specific VDAC regulation in cells of given organisms. For instance, PcVDAC32 selectivity is modulated by stigmasterol but not by cholesterol, the sole mammalian membrane sterol, and the PcVDAC32 voltage-dependence is inhibited at low ionic strengths that prevail in vivo [24], which is not observed for *Neurospora crassa* VDAC [26,32,33].

3. Structural Features

The three-dimensional (3-D) structures of mouse and human VDAC1 isoforms (mVDAC1 and hVDAC1, respectively) as well as of zebrafish VDAC2 isoform were determined at an atomic level using NMR, X-ray crystallography, or a combination of both the methods [34–37]. These isoforms form a large β-barrel-shaped pore made of 19 β-strands and one N-terminal segment folded into α-helix that is aligned almost parallel to the plane of the membrane at mid-height of the pore. Thus, the N-terminal segment creates a constriction in the central region of the pore. The results of solid-state NMR study confirms this orientation of the helix [38] and the propensity of the N-terminus to adopt an helical fold was shown by experimental and computational approaches [39,40]. It should be worth mentioning that these atomic resolution structures has been questioned [41,42] because they are not consistent with previously proposed empirical functional models. However, there are theoretical and experimental clues of their biological relevance [11,43–48].

As mentioned above, across different phylogenetic groups, VDAC amino acid sequences have a very low identity (≤5%) when considered as a whole but a relatively higher (≥25%) pairwise identity [11] suggesting that the protein sequences display common features. Firstly, they contain long stretches of alternating hydrophobic and hydrophilic amino acid residues typical of β-strands forming the β-barrel structure and a region with amino acid content characteristic for α-helix at N-terminus. Secondly, two conserved amino acid motifs have been detected close to C-terminus, namely the eukaryotic porin motif (PROSITE entry: PS00558) [49] and the β-motif regarded as essential for eukaryotic β-barrel protein import and assembly [50,51,52]. In addition, a motif specific to "green plants" (Viridiplantae) and located in N-terminal region has been identified [49]. Thus, VDAC proteins of different organisms might share a similar structure. For proper functioning of a hydrophilic pore formed by a transmembrane β-barrel protein a strict conservation of amino acids is not essential because the conservation of a proper arrangement of hydrophobic and hydrophilic residues should be suitable to preserve the β-barrel fold.

Spectroscopic studies indicate that VDAC proteins have the same secondary structure. Far-UV circular dichroism spectra of fungal, plant and human VDAC, solubilized in detergent, display negative extremum at 218 nm and positive peak at 195 nm, which are typical of β-pleated sheet [53–57]. The secondary structure of PcVDAC32, reconstituted in a planar lipid bilayer, was also investigated using the attenuated total reflection-Fourier transform infrared spectroscopy (ATR-FTIR). The results strongly indicate the occurrence of α-helix and antiparallel β-strands that are tilted by an angle of approximately 45 degrees and a proportion of amino acid residues involved in β-strand formation which is consistent with the three-dimensional structure data of mammalian VDAC1 [11,22]. Thus, comparative modelling based on mVDAC1 crystallographic and NMR studies was performed to build 3-D model of PcVDAC32 [11]. Normal mode analysis suggests that this 3-D model features a higher flexibility of β-strands 1 to 6 [11], in agreement with results of NMR studies [34,58], crystallographic B factor analysis and computational calculations [58] performed on the mammalian VDAC1. The electrostatic free energy profiles computed for the PcVDAC32 model and mVDAC1 crystal structure are similar and show that the transport of Cl^- is favored relative to that of K^+. Finally, for the PcVDAC32 model the distribution of the hydrophobic and charged amino acid residues are akin to those of mVDAC1 crystal structure. Notwithstanding these similarities, the structural model of PcVDAC32 must be treated as a working hypothesis to guide experiments and it must be tested against experimental results.

Substitutions of charged amino acid residues in the yeast *Saccharomyces cerevisiae* VDAC1 impact its selectivity indicating the major contribution of the electrostatic interactions to the VDAC selectivity [59]. The selectivity of *N. crassa* VDAC and PcVDAC32 are salt solution concentration-dependent [60,61]. This is a strong experimental evidence supporting the electrostatic contribution to the selectivity. A macroscopic one-compartment electrodiffusion model containing the effective fixed charge and the mobile ions diffusing inside the pore describes correctly PcVDAC32 selectivity [61]. The conductance and selectivity values computed from Brownian Dynamics (BD) simulations performed for the PcVDAC32 3-D model agree with the experimental data [61]. Interestingly, the concentration dependence of both selectivity and conductance measured for PcVDAC32 is fairly well describe by the BD simulation performed for mVDAC1 structure. Thus, the data suggest a conserved transport mechanism of ion transport.

4. Phaseolus VDAC Isoforms

Both *P. vulgaris* and *P. coccineus* belong to the same clade, which is relevant for comparative genomic and transcriptomic studies. We used genomic and transcriptomic data obtained for Andean landrace *P. vulgaris* [20] available at http://www.Phytozome.net/ to get further insight into *P. vulgaris* VDACs.

We found seven sequences described as *P. vulgaris* VDACs but not verified previously. Compared to other organisms, plants have a larger number of isoforms that reflects their molecular complexity. Whereas the origin of this complexity is still elusive there are some clues suggesting that this diversity might be correlated to more specific protein-protein interactions and isoform-specific functions [62]. Plants are sessile organisms that must face various biotic and abiotic stresses. Therefore, we might hypothesize that selective pressures associated with plant stress defenses have led to some VDAC isoform specificities after gene duplication. Moreover, a differential expression pattern of VDAC isoforms has been shown in different plant tissues [11], which suggests that another reason for functional specificities might be related to tissues specificities.

The theoretical physicochemical properties of the encoded protein sequences (named here PvVDAC1–PvVDAC7), supplemented by those of PcVDAC32, are summarized in Table 2.

The sequences of PvVDAC6 and PvVDAC7 are significantly shorter than the other ones. Moreover, the net charge of PvVDAC6 is negative whereas PvVDAC1–4, PvVDAC7 and PcVDAC32 have a positive net charge, which is consistent with anionic selectivity of VDAC in the open state. In agreement with experimental results [21], the predicted proteins with exception of PvVDAC6, have basic pI. The theoretical pI for PcVDAC32 is similar to the experimental value (pI = 8.8) [21]. The Gravy score (a measure of the average hydrophobicity) for the studied proteins is negative that is a typical feature of hydrophilic proteins. This is also observed for bacterial porins and β-barrel proteins of the chloroplast envelop [64]. It is due to the low content of hydrophobic residues, which are required in transmembrane β-barrel proteins to interact with membrane lipids (one out of two in transmembrane β-strands).

The phylogenetic tree generated for the predicted PvVDAC proteins contains three main clusters (Figure 4). The pairwise distances separating the sequences are given in Table 3. PcVDAC32 and PvVDAC4 are located very closely to each other and their sequences display 98% identity (99% similarity) whereas PvVDAC4 and PvVDAC5 sequences share 74% identity (88% similarity). In the most distant group, PvVDAC6 and PvVDAC7 sequences have 55% identity (74%

similarity). When compared with PcVDAC32, both PvVDAC6 and PvVDAC7 display 36% identity (54% and 50% similarity, respectively). This denotes high amino acid sequence variability of putative PvVDAC proteins. Remarkably, a good correlation between the PvVDAC sequence clustering (Figure 4) and the corresponding transcript expression (Figure 5) seems to exist. PvVDAC5 and PvVDAC4 are highly expressed and the later display the highest expression. This reminds PcVDAC31 and PcVDAC32, the latter being three time more abundant [21]. It appears that organisms have at least one abundant canonical isoform of VDAC that shares similar electrophysiological properties and sequence similarities with its cognate isoform from mitochondria of other species. For instance, this is the case for the mammalian VDAC1, yeast VDAC1 and plant PcVDAC32. The high amino acid identity/similarity between PvVDAC4 and PcVDAC32 suggests that they have similar structure and consequently function. Furthermore, we might assume a close relationship between PcVDAC31 and PvVDAC5 because their N-terminal regions comprising thirty amino acids [VKGPGLYTDIGKRTRDLLFKDYQNDHKFTI] are identical and their pI are close to neutrality [21]. Other predicted PvVDAC proteins have a low level of their respective transcript expression. Interestingly, despite shorter sequences predicted for PcVDAC6-7, their transcript expression occurs, which suggests that they might have a function.

Table 2. The theoretical physicochemical properties of putative VDAC proteins encoded by VDAC genes detected in *P. vulgaris* genome (http://www.Phytozome.net/). The physicochemical data were computed with ProtParam [63].

Acronym	Locus Name	Uniprot	residues	MW (kD)	Net charge	pI	GRAVY
PvVDAC1	Phvul.003G146600	V7C9B6	276	29.9	4	8.87	–0.200
PvVDAC2	Phvul. 001G027200	V7CRT6	276	29.6	7	9.25	–0.230
PvVDAC3	Phvul.002G011300	V7CIJ8	275	29.0	7	9.30	–0.075
PvVDAC4	Phvul.008G043800	V7B117	275	29.6	2	8.58	–0.167
PvVDAC5	Phvul.003G069300	V7CA94	275	29.5	0	7.24	–0.177
PvVDAC6	Phvul.003G192600	V7CEK4	244	26.4	–2	6.48	0.011
PvVDAC7	Phvul.009G190000	V7AY50	246	26.9	3	8.53	–0.105
PcVDAC32		V7C9B6	275	29.6	2	8.58	–0.195

Table 3. Pairwise distance of the predicted *Phaseolus* VDAC sequences. On the top of the columns, each number corresponds to a given VDAC sequence.

	1	2	3	4	5	6	7	8
[1] PcVDAC32								
[2] PvVDAC1	0.796							
[3] PvVDAC2	0.759	0.927						
[4] PvVDAC3	0.689	0.796	0.525					
[5] PvVDAC4	0.022	0.796	0.768	0.706				
[6] PvVDAC5	0.278	0.815	0.885	0.796	0.289			
[7] PvVDAC6	0.844	1.129	1.285	1.142	0.864	0.825		
[8] PvVDAC7	0.835	1.183	1.156	1.142	0.844	0.938	0.592	

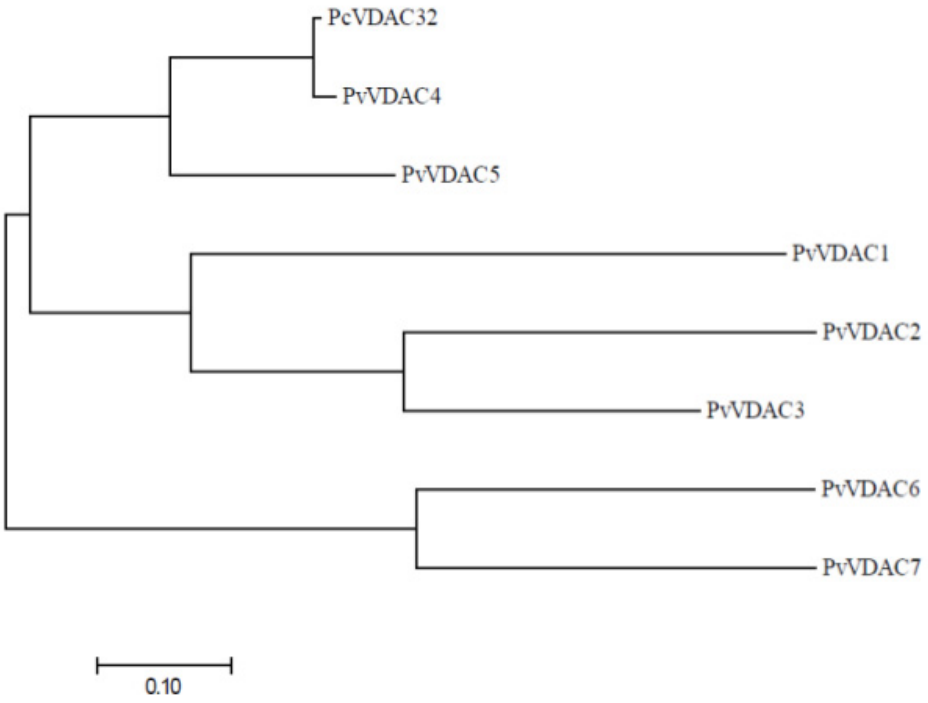

Figure 4. Neighbor-Joining phylogenetic tree built for putative *P.vulgaris* VDAC sequences and PcVDAC32. The bar (bottom of the figure) denotes the scale of the branch distance. The tree was generated with MEGA7 [65].

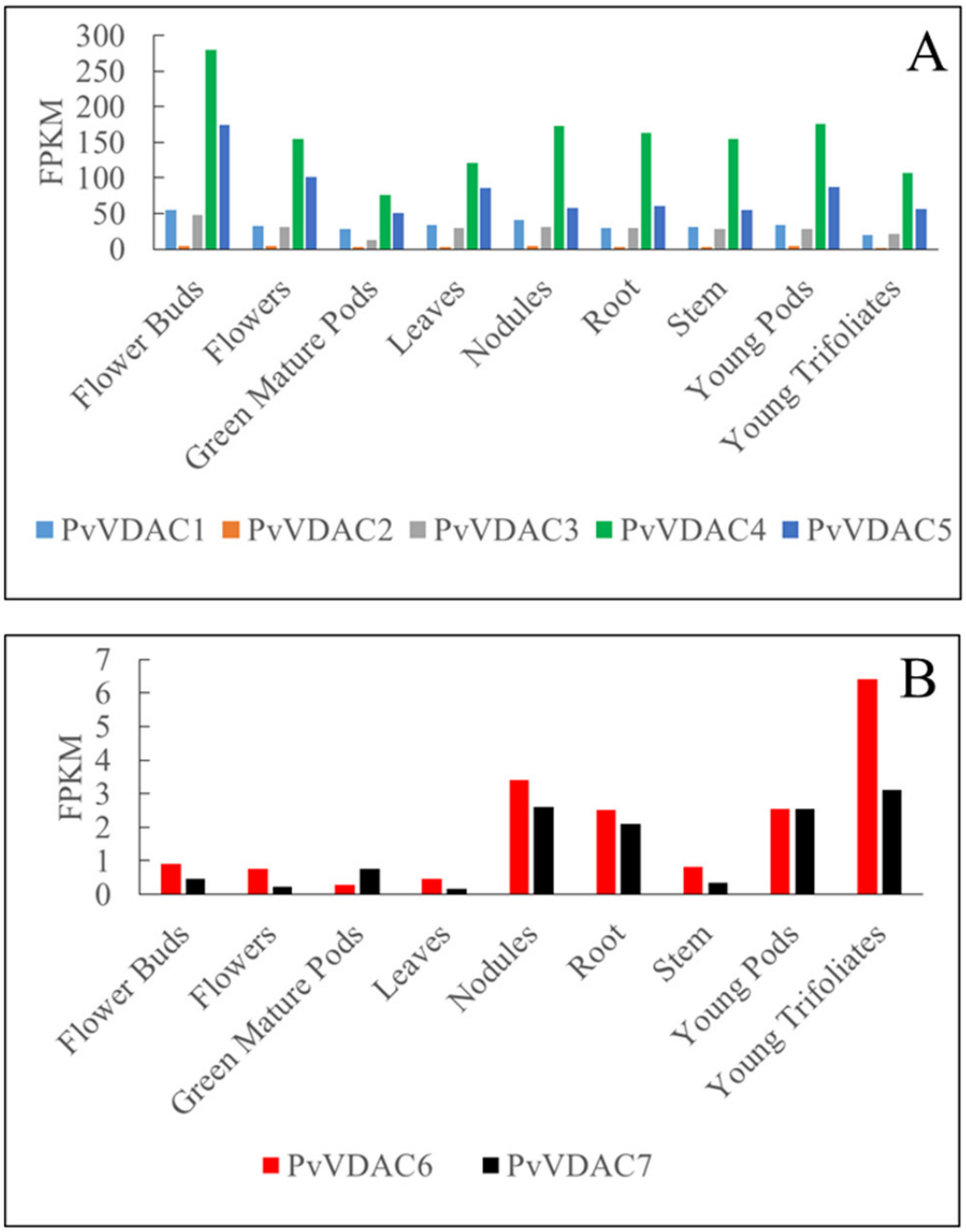

Figure 5. Relative expression of PvVDAC transcripts in different organs. The expression level is expressed in FPKM (Fragments Per Kilobase Million) units. The results are shown in two different panels because the expression level for PvVDAC6–7 (panel B) is much lower than that of PvVDAC1–5 (panel A). Data source: http://www.Phytozome.net/.

Multiple sequence alignment of VDAC sequences from different organisms (Figure S1) confirms the presence of VDAC conserved motifs [49]. As mentioned in § 3 (Structural features), two conserved amino acid motifs, namely the β motif [50] and the eukaryotic porin motif (EPM) are common for mitochondrial β-barrel proteins including VDAC proteins. The latter is the sorting

signal of mitochondrial β-barrel proteins. These two motifs are conserved in all the predicted PvVDAC proteins and in PcVDAC32 (Figure 6). Additionally, the Plant motif conserved in "green plants" [11,49] is also conserved in the studied sequences although in the case of PvVDAC6 and PvVDAC7 this motif is truncated at half of its length (Figure 7). Importantly, full sequences sharing an identity (≥80%) with PvVDAC6 or PvVDAC7 were also found for other genera, namely *Vigna angularis*, *Glycine max* and *Cajanus cajan* (Figure S2). They all belong to the same plant tribe (Phaseoleae) of the Faboideae, a subfamily of the Fabaceae, which explains the high identity score. As these sequences were found in different plant genera by independent laboratories, we can reasonably assume that these shorter sequences did not arise from a sequencing error.

Inside the EPM motif, the conserved pentapeptide VKA[K/R]V sequence has been proven to be essential for the assembly of yeast VDAC into MOM [66]. The EPM located at the C-terminus comprises 23 residues (Figure 6). In the sequence, the fifth residue is critical for targeting of *Arabidopsis thaliana* VDAC isoforms [67]. The position is occupied by residues P223, H223, P223 and Q221 in AtVDAC1, AtVDAC2, AtVDAC3 and AtVDAC4, respectively. Only proteins harboring proline at this position are exclusively targeted toward mitochondria [67]. With the exception of PvVDAC3, the other PvVDAC proteins contain proline at this critical position (Figure 8). In PcVDAC3, the proline residue is substituted for serine. This is a conservative substitution so we might expect that all the bean isoforms are targeted toward MOM.

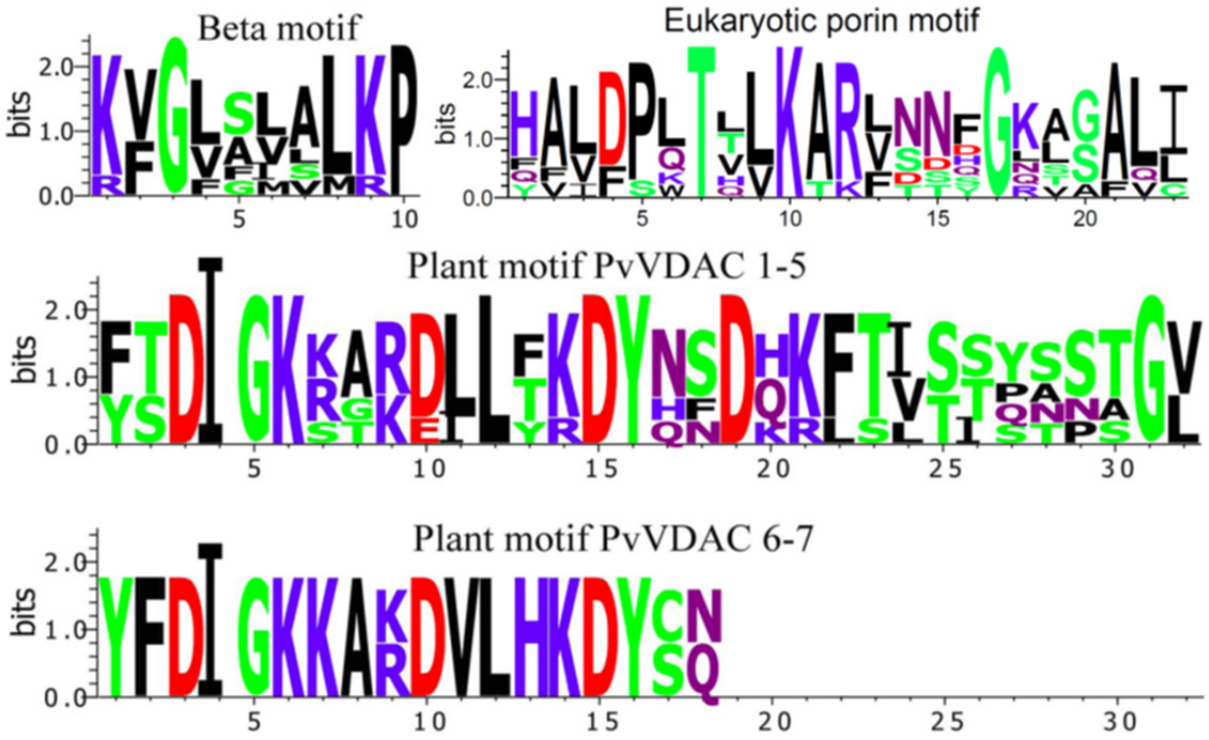

Figure 6. Logo representation of motifs found for the predicted PvVDAC proteins after multiple sequence alignment with MUSCLE [68]. The graphical representation of the motif sequences were done with WebLogo 3.5 [69,70]. The position of the motifs in the multiple sequence alignment is: plant motif 9-40, eukaryotic porin sequence 229–252 and β-motif 278–288.

```
          1        10        20        30        40        50        60
PvVDAC6   -MSTTPGIYFDIGKKAKDVLHKDYSN--------------------------LSPIHFH
PvVDAC7   -MNQGPGLYFDIGKKARDVLHKDYCQ--------------------------QPPIHFN
PvVDAC1   -MANGPAPFSDIGKRAKELLYKDYNFDHKFSLSIPNSTGLGLIATGLKKDQVFVGDISTL
PvVDAC5   -MVKGPGLYTDIGKRTRDLLFKDYQNDHKFTITTQTSTGVEITSTGVRKGELYLADISTK
PvVDAC4   -MAKGPGLYTDIGKKARDLLFKDYHSDQKFTVTTYSPTGVAITSSGTRKGELFVADVNTQ
PcVDAC32  -MAKGPGLYTDIGKKARDLLFKDYHSDQKFTVTTYSPTGVAITSSGTRKGELFLADVNTQ
PvVDAC2   MSGKGPGFFSDIGKSGRDILTKDYNSDQRFTISSSANSGLDLKSTLVKSRGLSSGDVTTE
PvVDAC3   -MSKGPGLFTDIGKKAKDLLTRDYNSDKKLTVSSYSSAGVALTSTAVKKGGVSTGDVAAL
```

Figure 7. N-terminus sequence of the predicted Phaseolus VDAC proteins showing the missing 27 amino acids in PvVDAC6 and PvVDAC7. The sequences were aligned with MUSCLE [68]. The Plant motif extends from position 9 to 40.

```
PvVDAC1   HALDPLTHLKARVNNYGLASALI
PvVDAC2   QFIDPKTVLKTRFSDDGKAAFQC
PvVDAC3   YVVDSQTVLKAKLNNHGNLGALL
PvVDAC4   HALFPQTLVKARFDTFGKAGAVI
PvVDAC5   HALDPLTTLKARVTNFGKTSALI
PvVDAC6   FAVDPLTQVKARLNNQGQLGALL
PvVDAC7   HALFPWTLLKARLSSSGRVGALI
PcVDAC32  HALDPLTTLKARVNNFGKSSALI
```

Figure 8. Eukaryotic porin motif (EPM) within the predicted PvVDAC proteins. The fifth residue critical for the protein targeting is shown in bold red. The sequence in bold blue is pentapeptide sequence essential for the assembly of yeast VDAC in MOM.

We have already mentioned here that PcVDAC32 is structurally and functionally similar to mammalian VDAC1. To assess whether predicted PvVDAC proteins might fold like mammalian VDAC1 we applied homology modelling, which is a method of choice to generate 3-D model of a protein of known amino acid sequence. For this purpose we used the SWISS-MODEL available at http://swissmodel.expasy.org/ [71]. The 3-D structure model was generated using mVDAC1 X-ray structure (3emn) as a template (Figure 9). The backbone of the model generated with PvVDAC1–5 and PcVDAC32 sequences is consistent with that of mVDAC1 3-D structure. However, both PvVDAC6 and PvVDAC7 models are at odds with mVDAC1 structure developed by crystallography.

The missing amino acid residues in PvVDAC6 and PvVDAC7 start at position 25 of their sequences viz. about the beginning of the first transmembrane β-strands indicating that the conformation of these two isoforms may significantly differ from the experimental 3-D structures. We resorted to the SPARK^{X} fold recognition method [72] to generate their putative folding patterns (Figure 10A). The results indicate that four β-strands at N-terminus are disrupted in both PvVDAC6 and PvVDAC7. Additionally, for PvVDAC7, the first predicted β-strand is too short (three predicted residues) to form a transmembrane segment. Taking into account the 19 β-strands proposed the

mammalian VDAC1, this suggests that the maximal number of β-strands in PvVDAC6 and PvVDAC7 structure might be 15 and 14, respectively. The number of residues between the first and last β-strands (7 and 9 residues, respectively) in PvVDAC6 or between the second and the last β-strands (8 and 9 residues, respectively) in PvVDAC7 should be sufficient to close properly the barrel. We noticed that the position of the N-terminal α-helix in both isoforms perfectly matched that of the mVDAC1 3-D structure (Figure 10B). Moreover, the three key residues involved in the main energy barrier for the inorganic ions and metabolites permeation are conserved and point toward the diffusion pore. Thus, this suggests that the helix might have a similar function in all PvVDAC isoforms.

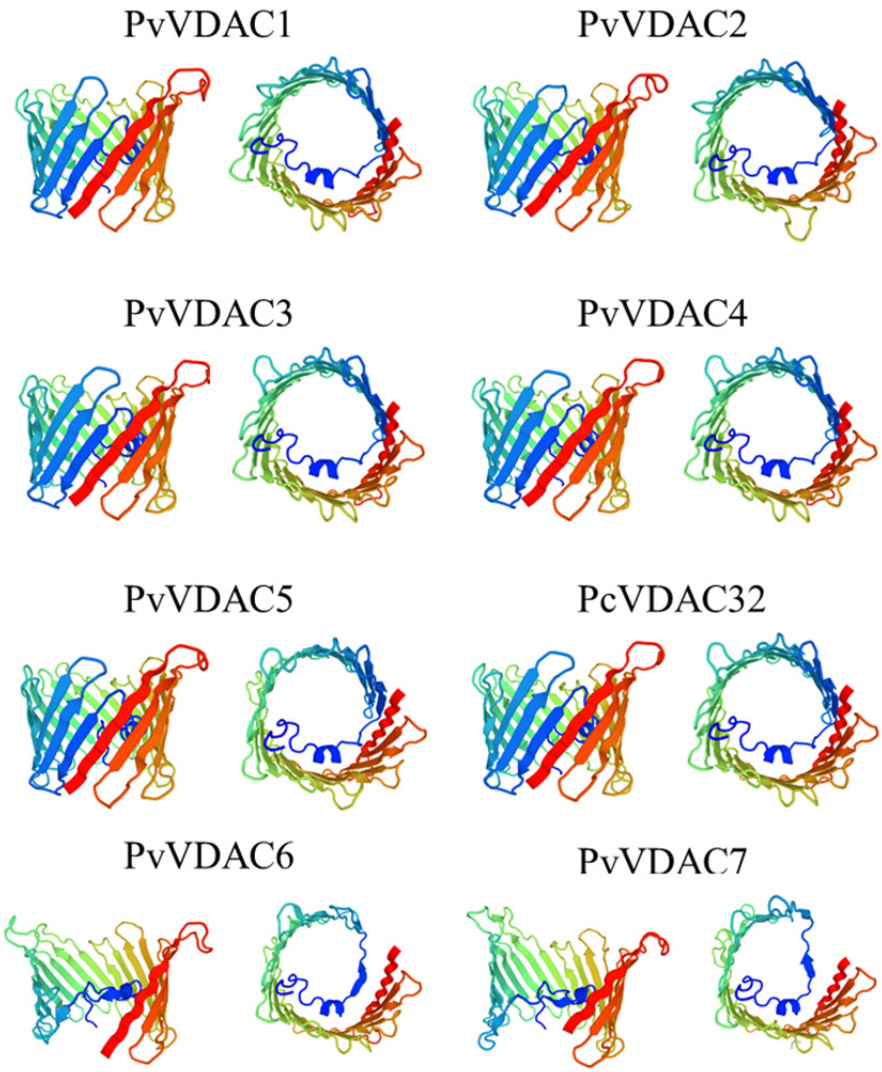

Figure 9. Putative 3-D models of the predicted *P. vulgaris* VDAC proteins. The models were generated using the SWISS-MODEL and mVDAC1 X-ray 3-D structure (3emn) as a template. For each VDAC a ribbon representation view parallel (left) or perpendicular (right) to the plane of the membrane is shown. In the parallel view the β-strand 1 (blue) and 19 (red) are side by side.

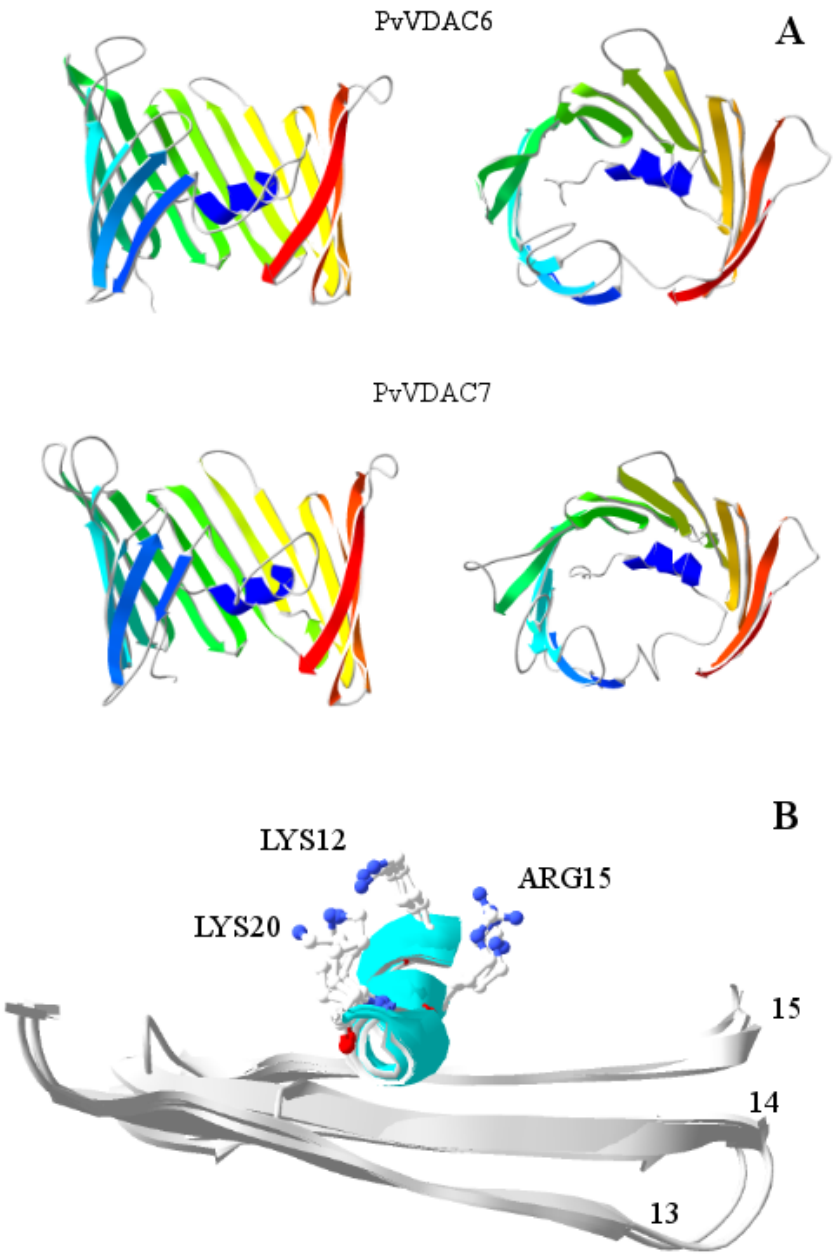

Figure 10. Putative 3-D models of the PvVDAC6 and PvVDAC7. (A) Ribbon representation view parallel (left) or perpendicular (right) to the plane of the membrane showing the predicted secondary structure. In the parallel view the first (blue) and last (red) β-strands are side by side. (B) Superposition of the PvVDAC6 and PvVDAC7 model structures and 3-D mVDAC1 structure (3emn) showing the conserved position of α-helix. The three positively charged residues involved in the main energy barrier for solute permeation is shown in the standard "ball and stick" representation. The number attached on the right side of each strand corresponds to the numbering of the 3emn structure. The PvVDAC structure models were generated with SPARK^{X} fold recognition method (http://sparks-lab.org/yueyang/server/SPARKS-X/).

Knowing that genes encoding PvVDAC6 and PvVDAC7 are expressed in plants (at least at the mRNA level) and that their predicted amino acid sequences include motifs conserved in mitochondrial β-barrel proteins (including a partial green plant VDAC motif) we can reasonably assume that the protein might adopt a β-barrel fold. The lower number of β-strands forming the pore will produced a barrel with a wall-to-wall diameter shorter (~2.5 nm) than the canonical VDAC (3.5 nm) [46]. We can thus anticipate that PvVDAC6 and PvVDAC7 might have a significantly different function than other PvVDACs. The issue of how these two proteins are folded and whether they have channel activity similar to VDAC is now open.

5. Conclusions

Our current knowledge of structure-function relationships in the case of plant VDAC proteins is mainly based on data obtained for PcVDAC32 from *P. coccineus*. However, although two PcVDAC isoforms are known to be expressed in *P. coccineus* seeds, little is known about the number of plant VDAC isoforms and their role in plant cell physiology. In this respect, seven putative VDAC encoding sequences termed here PvVDAC1–7 are found in the genome of *P. vulgaris*. PvVDAC4 has numerous properties similar to those of PcVDAC32, which suggests that they have similar structure and function. PvVDAC5 seems to be similar to PcVDAC31 and might have similar electrophysiological properties. PvVDAC1–3 sequences share structural similarities with the canonical VDAC found in plants, algae, fungi and animals. We can therefore assume that they belong to the VDAC family. The high expression of PvVDAC4 and PvVDAC5 transcripts suggests that the encoded proteins might be purified from mitochondria. The other ones would probably require the use of an efficient heterologous expression model that preserve the native protein properties. The sequences termed as PvVDAC6 and PvVDAC7 are shorter, and could form a β-barrel but with a smaller number of β-strands. Therefore, their annotation as members of the VDAC family should be subject to caution. This overview of *Phaseolus vulgaris* VDAC putative proteins highlights new information on their structure and function. Notably, their structural and/or functional similarities with VDAC of other plants pave the way for future research aiming at deciphering their role in plant physiology.

Acknowledgments

This work was supported by FRS-FNRS/PAN JOINT RESEARCH PROJECT. HK and FH are the project coordinators for Poland and Belgium, respectively. F.H. is a Research Director from the FRS-FNRS (Belgium).

Conflicts of Interest

All authors declare no conflicts of interest in this paper.

References

1. Delgado-Salinas A, Bibler R, Lavin M (2006) Phylogeny of the genus phaseolus (leguminosae): a recent diversification in an ancient landscape. *Syst Bot* 31: 779–791.

2. Chacón S MI, Pickersgill B, Debouck DG, et al. (2007) Phylogeographic analysis of the chloroplast DNA variation in wild common bean (Phaseolus vulgaris L.) in the Americas. *Plant Syst Evol* 266: 175–195.
3. Parreira JR, Bouraada J, Fitzpatrick MA, et al. (2016) Differential proteomics reveals the hallmarks of seed development in common bean (Phaseolus vulgaris L.). *J Proteomics* 143: 188–198.
4. Woodstock LW, Pollock BM (1965) Physiological predetermination: imbibition, respiration, and growth of lima bean seeds. *Science* 150: 1031–1032.
5. Palmieri F, Agrimi G, Blanco E, et al. (2006) Identification of mitochondrial carriers in Saccharomyces cerevisiae by transport assay of reconstituted recombinant proteins. *Biochim Biophys Acta* 1757: 1249–1262.
6. Inoue I, Nagase H, Kishi K, et al. (1991) ATP-sensitive K^+ channel in the mitochondrial inner membrane. *Nature* 352: 244–247.
7. Siemen D, Loupatatzis C, Borecky J, et al. (1999) $Ca2^+$-activated K channel of the BK-Type in the inner mitochondrial membrane of a human glioma cell line. *Biochem Biophys Res Commun* 257: 549–554.
8. Szabò I, Bock J, Jekle A, et al. (2005) A novel potassium channel in lymphocyte mitochondria. *J Biol Chem* 280: 12790–12798.
9. Pang K, Li Y, Liu M, et al. (2013) Inventory and general analysis of the ATP-binding cassette (ABC) gene superfamily in maize (Zea mays L.). *Gene* 526: 411–428.
10. Srinivasan V, Pierik AJ, Lill R (2014) Crystal structures of nucleotide-free and glutathione-bound mitochondrial ABC transporter atm1. *Science* 343: 1137–1140.
11. Homblé F, Krammer E-M, Prévost M (2012) Plant VDAC: Facts and speculations. *Biochim Biophys Acta-Biomembr* 1818: 1486–1501.
12. Marmagne A, Rouet M-A, Ferro M, et al. (2004) Identification of new intrinsic proteins in Arabidopsis plasma membrane proteome. *Mol Cell Proteomics* 3: 675–691.
13. Robert N, D'Erfurth I, Marmagne A, et al. (2012) Voltage-dependent-anion-channels (VDACs) in Arabidopsis have a dual localization in the cell but show a distinct role in mitochondria. *Plant Mol Biol* 78: 431–446.
14. De Pinto V, Messina A, Lane DJR, et al. (2010) Voltage-dependent anion-selective channel (VDAC) in the plasma membrane. *FEBS Lett* 584: 1793–1799.
15. Shoshan-Barmatz V, Pinto V De, Zweckstetter M, et al. (2010) VDAC, a multi-functional mitochondrial protein regulating cell life and death. *Mol Aspects Med* 31: 227–285.
16. Baker MA, Lane DJR, Ly JD, et al. (2004) VDAC1 is a transplasma membrane NADH-ferricyanide reductase. *J Biol Chem* 279: 4811–4819.
17. Parsons DF, Bonner J, Verboon JG (1965) Electron microscopy of isolated plant mitochondria and plastids using both the thin-section and the negative-staining techniques. *Can J Bot* 43: 647–655.
18. Mannella CA, Bonner WD (1975) X-ray diffraction from oriented outer mitochondrial membranes. *Biochim Biophys Acta-Biomembr* 413: 226–233.
19. Zalman LS, Nikaido H, Kagawa Y (1980) Mitochondrial outer membrane contains a protein producing nonspecific diffusion channels. *J Biol Chem* 255: 1771–1774.
20. Schmutz J, McClean PE, Mamidi S, et al. (2014) A reference genome for common bean and genome-wide analysis of dual domestications. *Nat Genet* 46: 707–713.

21. Abrecht H, Wattiez R, Ruysschaert JM, et al. (2000) Purification and characterization of two voltage-dependent anion channel isoforms from plant seeds. *Plant Physiol* 124: 1181–1190.
22. Abrecht H, Goormaghtigh E, Ruysschaert JM, et al. (2000) Structure and orientation of two voltage-dependent anion-selective channel isoforms—An attenuated total reflection Fourier-transform infrared spectroscopy study. *J Biol Chem* 275: 40992–40999.
23. Homblé F, Mlayeh L, Léonetti M (2010) Planar lipid bilayers for electrophysiology of membrane-active peptides, In: *Membr Pept Methods Results Struct Funct Electrophysiol,* IUL: La Jolla, 273–307.
24. Mlayeh L, Chatkaew S, Léonetti M, et al. (2010) Modulation of plant mitochondrial VDAC by phytosterols. *Biophys J* 99: 2097–2106.
25. Schein SJ, Colombini M, Finkelstein A (1976) Reconstitution in planar lipid bilayers of a voltage-dependent anion-selective channel obtained from paramecium mitochondria. *J Membr Biol* 30: 99–120.
26. Rostovtseva TK, Colombini M (1996) ATP flux is controlled by a voltage-gated channel from the mitochondrial outer membrane. *J Biol Chem* 271: 28006–28008.
27. Schmid A, Kromer S, Heldt HW, et al. (1992) Identification of two general diffusion channels in the outer membrane of pea mitochondria. *Biochim Biophys Acta* 1112: 174–180.
28. Heins L, Mentzel H, Schmid A, et al. (1994) Biochemical, molecular, and functional characterization of porin isoforms from potato mitochondria. *J Biol Chem* 269: 26402–26410.
29. Blumenthal A, Kahn K, Beja O, et al. (1993) Purification and characterization of the voltage-dependent anion-selective channel protein from wheat mitochondrial membranes. *Plant Physiol* 101: 579–587.
30. Smack DP, Colombini M (1985) Voltage-dependent channels found in the membrane fraction of corn mitochondria. *Plant Physiol* 79: 1094–1097.
31. Aljamal JA, Genchi G, De Pinto V, et al. (1993) Purification and characterization of porin from corn (Zea mays L.) mitochondria. *Plant Physiol* 102: 615–621.
32. Wunder UR, Colombini M (1991) Patch clamping VDAC in liposomes containing whole mitochondrial membranes. *J Membr Biol* 123: 83–91.
33. Levadny V, Colombini M, Li XX, et al. (2002) Electrostatics explains the shift in VDAC gating with salt activity gradient. *Biophys J* 82: 1773–1783.
34. Bayrhuber M, Meins T, Habeck M, et al. (2008) Structure of the human voltage-dependent anion channel. *Proc Natl Acad Sci USA* 105: 15370–15375.
35. Hiller S, Garces RG, Malia TJ, et al. (2008) Solution structure of the integral human membrane protein VDAC-1 in detergent micelles. *Science* 321: 1206–1210.
36. Ujwal R, Cascio D, Colletier JP, et al. (2008) The crystal structure of mouse VDAC1 at 2.3 A resolution reveals mechanistic insights into metabolite gating. *Proc Natl Acad Sci USA* 105: 17742–17747.
37. Schredelseker J, Paz A, Lopez CJ, et al. (2014) High resolution structure and double electron-electron resonance of the zebrafish voltage-dependent anion channel 2 reveal an oligomeric population. *J Biol Chem* 289: 12566–12577.
38. Schneider R, Etzkorn M, Giller K, et al. (2010) The native conformation of the human VDAC1 N terminus. *Angew Chemie Int Ed* 49: 1882–1885.
39. Guardiani C, Scorciapino MA, Amodeo GF, et al. (2015) The N-terminal peptides of the three human isoforms of the mitochondrial voltage-dependent anion channel have different helical

propensities. *Biochemistry* 54: 5646–5656.
40. De Pinto V, Tomasello F, Messina A, et al. (2007) Determination of the conformation of the human VDAC1 N-terminal peptide, a protein moiety essential for the functional properties of the pore. *Chem Bio Chem* 8: 744–756.
41. Colombini M (2009) The published 3D structure of the VDAC channel: native or not? *Trends Biochem Sci* 34: 382–389.
42. Colombini M (2012) VDAC structure, selectivity, and dynamics. *Biochim Biophys Acta-Biomembr* 1818: 1457–1465.
43. Lee K Il, Rui H, Pastor RW, et al. (2011) Brownian dynamics simulations of ion transport through the VDAC. *Biophys J* 100: 611–619.
44. Choudhary OP, Ujwal R, Kowallis W, et al. (2010) The electrostatics of VDAC: implications for selectivity and gating. *J Mol Biol* 396: 580–592.
45. Choudhary OP, Paz A, Adelman JL, et al. (2014) Structure-guided simulations illuminate the mechanism of ATP transport through VDAC1. *Nat Struct Mol Biol* 21: 626–632.
46. Hiller S, Abramson J, Mannella C, et al. (2010) The 3D structures of VDAC represent a native conformation. *Trends Biochem Sci* 35: 514–521.
47. Noskov SY, Rostovtseva TK, Bezrukov SM (2013) ATP Transport through VDAC and the VDAC-tubulin complex probed by equilibrium and nonequilibrium MD simulations. *Biochemistry* 52: 9246–9256.
48. Rui H, Lee K Il, Pastor RW, et al. (2011) Molecular dynamics studies of ion permeation in VDAC. *Biophys J* 100: 602–610.
49. Young MJ, Bay DC, Hausner G, et al. (2007) The evolutionary history of mitochondrial porins. *BMC Evol Biol* 7: 31.
50. Kutik S, Stojanovski D, Becker L, et al. (2008) Dissecting membrane insertion of mitochondrial beta-barrel proteins. *Cell* 132: 1011–1024.
51. Imai K, Fujita N, Gromiha MM, et al. (2011) Eukaryote-wide sequence analysis of mitochondrial beta-barrel outer membrane proteins. *BMC Genomics* 12: 79.
52. Jores T, Klinger A, Grosz LE, et al. (2016) Characterization of the targeting signal in mitochondrial [beta]-barrel proteins. *Nat Commun* 7.
53. Shanmugavadivu B, Apell HJ, Meins T, et al. (2007) Correct folding of the beta-barrel of the human membrane protein VDAC requires a lipid bilayer. *J Mol Biol* 368: 66–78.
54. Shi Y, Jiang C, Chen Q, et al. (2003) One-step on-column affinity refolding purification and functional analysis of recombinant human VDAC1. *Biochem Biophys Res Commun* 303: 475–482.
55. Koppel DA, Kinnally KW, Masters P, et al. (1998) Bacterial expression and characterization of the mitochondrial outer membrane channel. Effects of n-terminal modifications. *J Biol Chem* 273: 13794–13800.
56. Shao L, Kinnally KW, Mannella CA (1996) Circular dichroism studies of the mitochondrial channel, VDAC, from *Neurospora crassa*. *Biophys J* 71: 778–786.
57. Smeyers M, Léonetti M, Goormaghtigh E, et al. (2003) Structure and function of plant membrane ion channels reconstituted in planar lipid bilayers, In: *Membr Sci Technol—Planar lipid bilayers their appl,* Elsevier, 449–478.
58. Villinger S, Briones R, Giller K, et al. (2010) Functional dynamics in the voltage-dependent anion channel. *Proc Natl Acad Sci* 107: 22546–22551.

59. Blachly-Dyson E, Peng S, Colombini M, et al. (1990) Selectivity changes in site-directed mutants of the VDAC ion channel: structural implications. *Science* 247: 1233–1236.
60. Zambrowicz EB, Colombini M (1993) Zero-current potentials in a large membrane channel: a simple theory accounts for complex behavior. *Biophys J* 65: 1093–1100.
61. Krammer E-M, Saidani H, Prévost M, et al. (2014) Origin of ion selectivity in *Phaseolus coccineus* VDAC mitochondrial channel. *Mitochondrion* 19B: 206–213.
62. Rosenquist M, Sehnke P, Ferl RJ, et al. (2000) Evolution of the 14-3-3 protein family: does the large number of isoforms in multicellular organisms reflect functional specificity? *J Mol Evol* 51: 446–458.
63. Gasteiger E, Hoogland C, Gattiker A, et al. (2005) Protein identification and analysis tools on the ExPASy server, In: Walker JM, *Proteomics Protoc,* Totowa: Humana Press, 571–607
64. Schleiff E, Eichacker LA, Eckart K, et al. (2003) Prediction of the plant beta-barrel proteome: A case study of the chloroplast outer envelope. *Protein Sci* 12: 748–759.
65. Kumar S, Stecher G, Tamura K (2016) MEGA7: molecular evolutionary genetics analysis version 7.0 for bigger datasets. *Mol Biol Evol* 33.
66. Smith MD, Petrak M, Boucher PD, et al. (1995) Lysine residues at positions 234 and 236 in yeast porin are involved in its assembly into the mitochondrial outer membrane. *J Biol Chem* 270: 28331–28336.
67. Tateda C, Watanabe K, Kusano T, et al. (2011) Molecular and genetic characterization of the gene family encoding the voltage-dependent anion channel in Arabidopsis. *J Exp Bot* 62: 4773–4785.
68. Edgar RC (2004) MUSCLE: multiple sequence alignment with high accuracy and high throughput. *Nucleic Acids Res* 32: 1792–1797.
69. Schneider TD, Stephens RM (1990) Sequence logos: a new way to display consensus sequences. *Nucleic Acids Res* 18: 6097–6100.
70. Crooks GE, Hon G, Chandonia J-M, et al. (2004) WebLogo: a sequence logo generator. *Genome Res* 14: 1188–1190.
71. Biasini M, Bienert S, Waterhouse A, et al. (2014) SWISS-MODEL: modelling protein tertiary and quaternary structure using evolutionary information. *Nucleic Acids Res* 42: W252–W258.
72. Yang Y, Faraggi E, Zhao H, et al. (2011) Improving protein fold recognition and template-based modeling by employing probabilistic-based matching between predicted one-dimensional structural properties of query and corresponding native properties of templates. *Bioinformatics* 27: 2076–2082.

AIMS Press